Journal of Water & Health

IWA PUBLISHING

Journal of Water and Health Vol 21 No 9, 1242 doi: 10.2166/wh.2023.128

Modeled and measured SARS-CoV-2 virus in septic tank systems for wastewater surveillance

Dong Li [a], Hunter Quon [b,c], Jared Ervin [d], Sunny Jiang [b,c], Diego Rosso [b,c], Laurie C. Van De Werfhorst [a], Brandon Steets [d] and Patricia A. Holden [a,*]

[a] Bren School of Environmental Science & Management, University of California, Santa Barbara, CA 93016, USA
[b] Department of Civil and Environmental Engineering, University of California, Irvine, CA 92697-2175, USA
[c] Water-Energy Nexus Center, University of California, Irvine, CA 92697-2175, USA
[d] Geosyntec Consultants, Santa Barbara, CA 93101, USA
*Corresponding author. E-mail: holden@bren.ucsb.edu

DL, 0000-0001-9990-7742; PAH, 0000-0002-6777-5359

ABSTRACT

SARS-CoV-2 wastewater surveillance (WWS) at wastewater treatment plants (WWTPs) can reveal sewered community COVID-19 prevalence. For unsewered areas using septic tank systems (STSs) or holding tanks, how to conduct WWS remains unexplored. Here, two large STSs serving Zuma Beach (Malibu, CA) were studied. Supernatant and sludge SARS-CoV-2 concentrations from the directly-sampled STSs parameterized a dynamic solid–liquid separation, mass balance-based model for estimating the infection rate of users. Pumped septage before hauling and upon WWTP disposal was also sampled and assessed. Most (96%) STS sludge samples contained SARS-CoV-2 N1 and N2 genes, with concentrations exceeding the supernatant and increasing with depth while correlating with total suspended solids (TSS). The trucked septage contained N1 and N2 genes which decayed (coefficients: 0.09–0.29 h^{-1}) but remained detectable. Over approximately 5 months starting in December 2020, modeled COVID-19 prevalence estimations among users ranged from 8 to 18%, mirroring a larger metropolitan area for the first 2 months. The approaches herein can inform public health intervention and augment conventional WWS in that: (1) user infection rates for communal holding tanks are estimable and (2) pumped and hauled septage can be assayed to infer where disease is spreading in unsewered areas.

Key words: decay rate, depth profile, mass balance-based model, pepper mild mottle virus, SARS-CoV-2, septic system

HIGHLIGHTS

- Public communal septic systems were sampled over time for SARS-CoV-2.
- SARS-CoV-2 sludge concentrations exceeded supernatant and followed TSS.
- Sludge was sampleable during periodic disposal, but SARS-CoV-2 decayed while hauling.
- Mass balance-based modeling well represented SARS-CoV-2 loading into septic systems.
- The prevalence of COVID-19 infections was estimable.

GRAPHICAL ABSTRACT

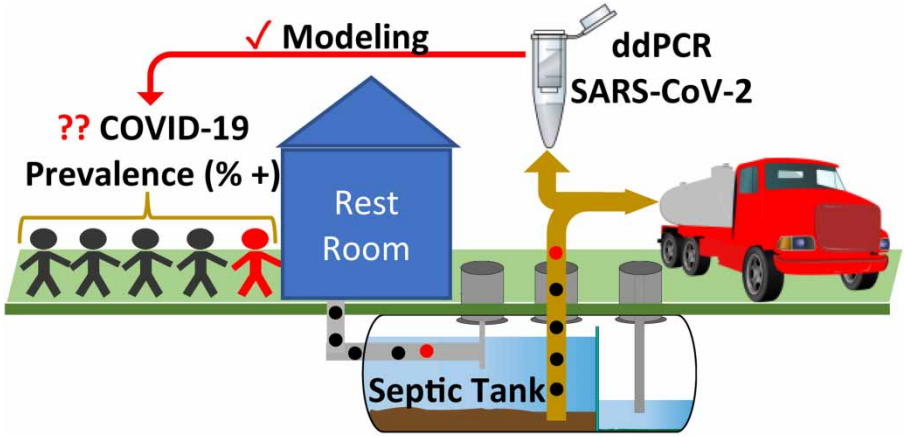

INTRODUCTION

The Coronavirus Disease-2019 (COVID-19) disease caused by severe acute respiratory syndrome coronavirus 2 (SARS-CoV-2) became a global pandemic. With COVID-19, patient-based clinical surveillance is complex because over 30% of infected individuals are asymptomatic (Nishiura *et al.* 2020). However, a significant amount of SARS-CoV-2 virus is shed with feces and other bodily fluids of both symptomatic and asymptomatic individuals (Kitajima *et al.* 2020; Nishiura *et al.* 2020), including after recovery (Zheng *et al.* 2020). As such, wastewater surveillance (WWS) of SARS-CoV-2 RNA in wastewater treatment plant (WWTP) influent (Kitajima *et al.* 2020) and primary sludge (Graham *et al.* 2020; Balboa *et al.* 2021; D'Aoust *et al.* 2021) can reflect community COVID-19 infections in areas equipped with sewers (Medema *et al.* 2020; Peccia *et al.* 2020; Diamond *et al.* 2022). Hence, WWS is now an established complement to local clinical surveillance in sewered areas. However, onsite wastewater treatment systems such as septic tank systems (STSs) are used in unsewered areas (U.S. EPA. 2002), with STSs serving approximately 25% or more of U.S. and European homes (U.S. EPA. 2002; Williams *et al.* 2012). STSs, in that they are periodically pumped, are also analogous to communal human waste holding tanks used widely in developing countries (Massoud *et al.* 2009). Yet, although SARS-CoV-2 RNA has been reported for STSs (Zhang *et al.* 2020; Iwamoto *et al.* 2022; Amin *et al.* 2023), relatively less is known regarding the distribution of SARS-CoV-2 and the potential for WWS from such systems.

Typically, STSs are comprised of a one- or two-chamber septic tank receiving wastewater from individual or small groups of dwellings that are not connected to a sewage collection system, with a downstream leach field for infiltration and further treatment of septic tank effluent (Withers *et al.* 2014; Lusk *et al.* 2017). Although STSs have been studied for effectiveness in treating household wastewater (Withers *et al.* 2014; Lusk *et al.* 2017) and human fecal viral persistence in leach fields (Ferguson *et al.* 2009), where and how to sample STSs or communal holding systems for SARS-CoV-2 has not been addressed (Haque *et al.* 2022), including if representative sampling can conveniently be performed during system pump-out as one of several possible stages of waste handling (Maqbool *et al.* 2022). Furthermore, the accumulation and fate of SARS-CoV-2 in STSs, for example in the septic tank sludge blanket layer, has not been explored, including for the relevance of concentrations to viral loading and how to use monitoring data from STSs for WWS. We hypothesized that the SARS-CoV-2 virus concentrates in settled septic tank solids, in comparison to the corresponding supernatant layer (Amin *et al.* 2023), because of the known affinity of the viral lipid-protein coat with organic particles (Kitajima *et al.* 2020). Therefore, a solid–liquid separation model based on a clarification-thickening process (Takács *et al.* 1991) should be applicable to STSs to estimate SARS-CoV-2 accumulation in the sludge layer prior to septic tank pumping. A descriptive tank reactor mass balance model applied to STSs has the potential to simulate the temporal pattern of infected contributing individuals based on the time course of viral loading in the sludge blanket.

Here, we asked how to best sample STSs, and how to relate SARS-CoV-2 concentrations to possible numbers of infected contributors. As model systems, STSs serving two high-use public restrooms located at Zuma Beach (Malibu, CA) were studied. Pepper mild mottle virus (PMMoV) RNA, which is prevalent in human feces, was used as a measure of 'fecal

strength' and to normalize SARS-CoV-2 RNA concentrations in the septage samples (D'Aoust *et al.* 2021). SARS-CoV-2 RNA concentrations were compared across the STSs, a hauling truck, and at the hauled material WWTP disposal point, to explore sampling feasibility and how viral decay could impinge on sampling location. A tank reactor mathematical model was developed for simulating the viral load into the sludge blanket. Although the model requires more testing to determine its applicability for STSs based on pump-out frequency, the model was used here to estimate the proportion of infected contributors among the directly counted total users. In this way, we provide a unique and transferable method for determining SARS-CoV-2 prevalence in unsewered areas that use STS-like wastewater management and that can be sampled directly: sample sludge and measure SARS-CoV-2 concentrations; measure sludge TSS; estimate or measure total flows into the STS plus the counts of persons contributing wastewater over a time interval; determine what COVID-19 disease prevalence (%) should be assumed such that model predictions of SARS-CoV-2 in sludge match actual measurements. For STS systems that cannot be sampled directly, we discuss the benefit of sampling from the hauled septage disposal point for informing community-based WWS. The results contribute to understanding SARS-CoV-2 in STSs of unsewered or rural areas affected by COVID-19, and the modeling method, plus sampling approaches, used in this study can be also applied to other pathogens to estimate infections in local populations.

MATERIALS AND METHODS

Sampling details

Zuma Beach is a popular public recreational beach, 2.9 km (1.8 mile) long, located in Malibu, CA, with 20,000 to 1,000,000 monthly visitations in 2019. There are nine public restroom (RR) facilities, of which two high-use facilities based on previous estimates of visitors and average water usage (data are not shown) were studied: RR#1 and RR#9, each with six showers, nine toilets, eight sinks, and three urinals, and each discharging into a dedicated STS (Supplementary material, Figure S1).

Supernatant and sludge were sampled approximately every other week (total 8 and 12 times from RR#1 and #9, respectively) from December 1, 2020, to May 4, 2021 (Supplementary material, Table S1). STS primary tank contents were observed to be stratified into three layers: floating scum, supernatant, and underlying sludge; scum was not sampled. Supernatant (i.e., liquid between scum layer and sludge) was routinely sampled from its mid-depth, overlying the sludge. Sludge was routinely sampled from the bottom of the primary tank at the port close to the tank middle. To enable understanding virus stratification across the supernatant and sludge depth profiles, RR#9 supernatant samples from the top and midpoint depths of the supernatant layer, and RR#9 sludge samples from the top and bottom depths of the sludge layer, were also collected on March 9 and 22, 2021. A pumping and hauling sub-study was carried out at the RR#9 STS when the system was pumped on March 22, 2021. RR#9 subsequently closed before the last two sampling events, due to a maintenance event. Thus, on April 20, 2021, the RR#9 sludge depth was too low to sample, and only supernatant samples from the midpoint and bottom depths were collected. Separate men's and women's visits of RR#9 were recorded using a people counting system (OmniCounter-ProA; Traf-Sys Co.) between January 26 and March 22, 2021 (Supplementary material, Table S1).

Septage hauling sub-study

On March 22, 2021, the septage in the RR#9 primary tank was pumped out by a commercial septage hauler and transported (2 h) before discharge to the Joint Water Pollution Control Plant (JWPCP) of the Sanitation Districts of Los Angeles County (Supplementary material, Figure S2). To assess septage sample representativeness from a septic hauler discharging to a WWTP – in comparison to sludge and supernatant sampled directly from an STS – and to assist quantifying SARS-CoV-2 RNA decay during hauling, sampling was conducted on the day of septic pumping at RR#9. Samples from four STS locations were collected: the top and bottom depths of the sludge layer prior to pumping; the top and midpoint depths of the supernatant layer prior to pumping; mixed samples (mixture of supernatant and sludge) from the truck immediately after pumping the primary tank; and mixed samples (mixture of supernatant and sludge) from the truck prior to discharge at JWPCP. The mixed septage samples in the truck prior to discharge were collected from the access hatches on the top of the truck, one from the rear, one from the middle, and one from the front of the truck; these mixed samples were analyzed separately. Additionally, heat-inactivated SARS-CoV-2 (VR-1986HK, ATCC) was spiked into six replicate septage subsamples of the mixed septage samples taken from the rear of the truck. Three spiked samples were put immediately on ice and the other three spiked samples were kept at ambient temperature (~70 °F in the dark) until arrival to the JWPCP WWTP. Viral RNA decay during hauling was evaluated by comparing SARS-CoV-2 RNA concentrations in septage samples collected from the truck just after pumping to those just prior to discharge, as well as using sludge samples spiked with heat-inactivated

SARS-CoV-2 kept on ice and at ambient temperature during transport. In this way, both intrinsic decay (of endogenous mixed septage SARS-CoV-2) and potential alteration of SARS-CoV-2 recovery (e.g., in case of hauling truck internal factors such as residual chemical additives) were assessable.

Sample and data analyses

Collected samples were transported on ice to the University of California, Santa Barbara within 3–6 h after sampling. The details of total suspended solids (TSS) measurement, sample archiving, RNA extraction, SARS-CoV-2 and PMMoV analyses, and statistical analyses are in the Supplementary material.

Septic tank general model for COVID-19 case estimation

The Zuma Beach RR#9 37.8 m^3 (10,000 gal) STS (Figure 1) is modeled as a tank reactor with ideal solid–liquid separation according to a dynamic clarification-thickening process (Takács *et al.* 1991). This ideal septic tank is divided into two layers: the supernatant and the sludge blanket. The system is modeled as a continuously stirred tank reactor (CSTR), assuming: (1) constant steady state volumetric inflow and outflow rates, with instantaneous mixing and uniform distribution of constituent concentrations throughout each layer and (2) mass transfer only occurring vertically from the top layer to the bottom layer based on gravitational settling. The model simulates the fate of constituents in between tank pump-out cycles. That is, at time $t = 0$ the tank is empty, and at time $t = t_f$ the tank will be emptied once again. Tank constituents are associated with specific reactive rates such as decay or growth. Thus, the general structure of this septic tank model approximates a reactive primary clarifier (Gernaey *et al.* 2001).

Viral loading sub-model

In the viral loading sub-model, virus accumulation and trends over the study period in an STS were modeled for only the sludge blanket layer and analyzed between septic pump-out cycles, since sludge accumulation is the primary criterion around which STSs are designed and periodically pumped out. Based on the above assumptions, a mass balance of virus for the sludge blanket layer was created as shown in Equation (1):

$$\frac{dZ_{sb}}{dt} = \phi\, r_g Q P Z_{in} - k_d Z_{sb}(t) \tag{1}$$

In Equation (1), Z_{sb} is the total number of viruses in the sludge blanket (genome copies, hereafter gc), ϕ is the fraction of viruses that partition to the solids in the wastewater (unitless), r_g is the fraction of readily settleable solids in the wastewater (unitless), Q is the wastewater inlet flowrate (l d^{-1}), P is the number of infected persons contributing to the viral load per day (person d^{-1}), Z_{in} (gc person^{-1} l^{-1}) is the virus concentration in the inlet wastewater flow calculated based on the shedding

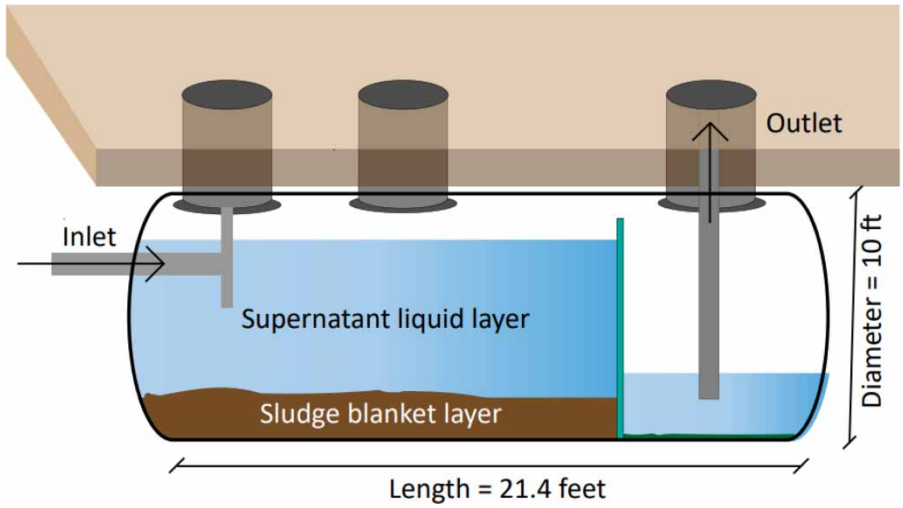

Figure 1 | Schematic diagram of the septic tank used to represent RR#9 in the model.

rate of infected individuals (see below for details), and k_d is the virus decay coefficient in wastewater (d^{-1}). The growth term in the reactor is zero.

The concentration of viruses in wastewater entering the septic tank was estimated based on clinical data of SARS-CoV-2 in feces of COVID-19 patients (Wölfel *et al.* 2020; Zheng *et al.* 2020). Since the virus shedding rate varies with the progression of the disease, there is a large range of SARS-CoV-2 genome concentration per volume of patient feces (Supplementary material, Table S2). The clinical data were first treated to unify the reporting unit as described in a previous study (Shi *et al.* 2021) and fitted by an empirical distribution curve (Supplementary material, Figure S3(a)). The empirical distribution curve for human fecal volume per day (Supplementary material, Figure S3(b)) was generated according to data collected by Wyman *et al.* (1978). Then, the concentrations of SARS-CoV-2 in toilet flushing water by each patient is calculated using Equation (2) by incorporating an average volume of toilet flushing water. Finally, viral loading to the RR#9 STS is computed using the total wastewater volumetric flowrate measured in the STS by Equation (3). The wastewater flowrate, Q, was estimated based on outflow pump measurements at the study site. These were collected intermittently; thus interpolation was used to estimate the amount of flow per day during the study period. A list of flowrate values for the entire period used in the model can be found in Supplementary material (Table S3).

$$C_{\text{virus,flush}} = C_{\text{virus,feces}} \times \frac{V_{\text{feces}}}{V_{\text{feces}} + V_{\text{flush}}} \tag{2}$$

$$Z_{\text{in}} = C_{\text{virus,flush}} \times \left(\frac{V_{\text{feces}} + V_{\text{flush}}}{V_{\text{feces}} + V_{\text{flush}} + V} \right) \tag{3}$$

Here, $C_{\text{virus,flush}}$ is the concentration of viruses in toilet flush water from an infected person (gc l^{-1}), $C_{\text{virus,feces}}$ is the concentration of viruses in human feces from an infected person (gc l^{-1}), V_{feces} is the human fecal volume per day (l d^{-1}), and V_{flush} is the volume of toilet flush water in one flush (l d^{-1}), and V is the total volume of flow into the septic tank in a 24-h period (l d^{-1}; equivalent to the varying Q multiplied by 1 d). Equations (2) and (3) estimate the virus input to the tank for each infected person who uses the RR each day. To capture the uncertainties of virus shedding at different stages of COVID-19 and daily fecal volumes, a Monte Carlo estimation was made using 10,000 iterations to produce a range of values for Z_{in} in MATLAB 2022a (MATLAB, Mathworks).

Equation (1) was then solved over a time domain of 272 days using MATLAB 2022a. This corresponds with the data collection ending in March 2021 and begins with the most recent time the tank was emptied of sludge, in August 2020. For estimation of total loading over the entire sludge volume, it was assumed that the sludge blanket geometry was that of a partially filled horizontal tank. For details regarding dimensions and the geometric equation, see the Supplementary material. A list of the parameters for Equations (1)–(3) and their respective values and sources are compiled in Table 1.

Table 1 | Parameter definitions and values for use in Equations (1)–(3)

Definition	Parameter	Value or distribution	Units	Source
Fraction of enveloped viruses that partitions to solids	ϕ	0.25	Unitless	Ye *et al.* (2016)
Gravitation settling coefficient (readily settleable fraction)	r_g	0.6	Unitless	Metcalf and Eddy, fifth Edition
Decay of SARS-CoV-2 in wastewater	k_d	0.17–1.4	d^{-1}	Ahmed *et al.* (2020); Bivins *et al.* (2020)
Volume of water per toilet flush	V_{flush}	4.85	l d^{-1}	CA Title 20
Human fecal volume per day	V_{feces}	Empirical distribution	l d^{-1}	Wyman *et al.* (1978)
Concentration of SARS-CoV-2 in infected human feces	$C_{\text{virus.feces}}$	Empirical distribution	gc l^{-1}	Wölfel *et al.* (2020); Zheng *et al.* (2020)

Estimation of infected individuals

The outputs of the model (Equation (1)) were used to capture the trends in both the sludge blanket viral loading and the potential rates of infected individuals (P) using RR#9 over time. As the virus shedding by individuals with COVID-19 is in units of per person per day (Equations (2) and (3)), the influx of virus can be scaled based on how many infected people are estimated to use the RR on a given day. The parameter P in Equation (1) represents this scale. The values of P were varied to best simulate the trends in the SARS-CoV-2 results for the samples collected in the sludge blanket. P was then used to represent prevalence of COVID-19 cases by Equation (4):

$$\text{Prevalence}_{\text{model}} = \frac{P}{\text{RR users}} \tag{4}$$

Here, the number of RR users was estimated and interpolated based on RR utilization rate according to the people counter data from RR#9 (Supplementary material, Table S3). As shown in Equation (4), the prevalence is defined as the fraction of infected individuals among the total RR users on that day.

To gage the credibility of model outputs, a sensitivity analysis was conducted to identify the model parameters in Equation (1) that had the greatest contribution to uncertainty and variability in the results. Using Monte Carlo simulation and 10,000 iterations of the input parameters, the Spearman rank correlation coefficient was computed in MATLAB to determine the strength and direction of a presumed monotonic relationship between input parameters and model output, where a coefficient of 0 indicates no influence of the variable on the results, and a value of ± 1 indicates a positive or negative influence on the output. The sensitivity analysis was conducted for the following parameters and uniform distributions: flowrate Q for U(10, 10,000; l d^{-1}, this study), virus attachment ϕ for U(0.22, 0.26) (Ye *et al.* 2016), virus decay rate k_d for U (0.17, 1.4; d^{-1}) (Ahmed *et al.* 2020; Bivins *et al.* 2020) and the number of infected RR users P for U (6, 42; this study).

Comparisons to local and regional COVID-19 cases

The Malibu city 7-day average daily infection case number was downloaded (http://publichealth.lacounty.gov/). Spearman correlation analyses were performed to test for significance and the strength of the correlation between SARS-CoV-2 RNA concentrations and infection case numbers, with a p value of 0.05 or lower signifying significance. The estimated COVID-19 prevalence in RR#9 was further compared with the prevalence reported by LA County during the same time period. The prevalence of infected individuals that shed SARS-CoV-2 in LA County is estimated using Equation (5):

$$\text{Prevalence}_{\text{county}} = \frac{4\sum_{i=1}^{14} \text{Reported cases}}{10^7} \times 100\% \tag{5}$$

The numerator of this equation estimates the 14-day moving sum of daily new cases, with i as SARS-CoV-2 fecal shedding days based on clinical data. A scaling factor of 4 was added according to the CDC estimation for disease burden from February 2020 to September 2021, in that only one in four cases were reported (CDC 2021). Finally, this moving sum of infections was divided by 10^7, the approximate population of LA County (https://www.census.gov/quickfacts/fact/table/losangelescountycalifornia/PST045221).

RESULTS

SARS-CoV-2 RNA in supernatant and sludge samples

The human RP gene was detected in all supernatant and sludge samples, with the exception of one RR#1 supernatant sample (Supplementary material, Table S1). The SARS-CoV-2 N1 gene was detected in 28.6% (2 of 7) RR#1 supernatant samples and the N2 gene in 85.7% (6 of 7) samples (Supplementary material, Figure S4 and Table S1). N1 and N2 genes were each detected in 26.3 and 100.0% (5 and 19 samples, respectively) of 19 RR#9 supernatant samples (Figure 2; Supplementary material, Table S1). N1 and N2 concentrations averaged 45.3 and 143.5 copies/mL, respectively, in positive RR#1 supernatant samples; and 78.7 and 124.9 copies/mL, respectively, in positive RR#9 supernatant. The N2 concentrations were significantly higher than those of N1 in all supernatant samples (Wilcoxon test, $p < 0.0001$, $n = 26$). For sludge samples, both N1 and N2 targets were detected in 85.7% (6 of 7) of RR#1 samples (Supplementary material, Figure S4) and 100.0% (all 17) of RR#9 samples (Figure 2; Supplementary material, Table S1). The highest N1 and N2 concentrations in

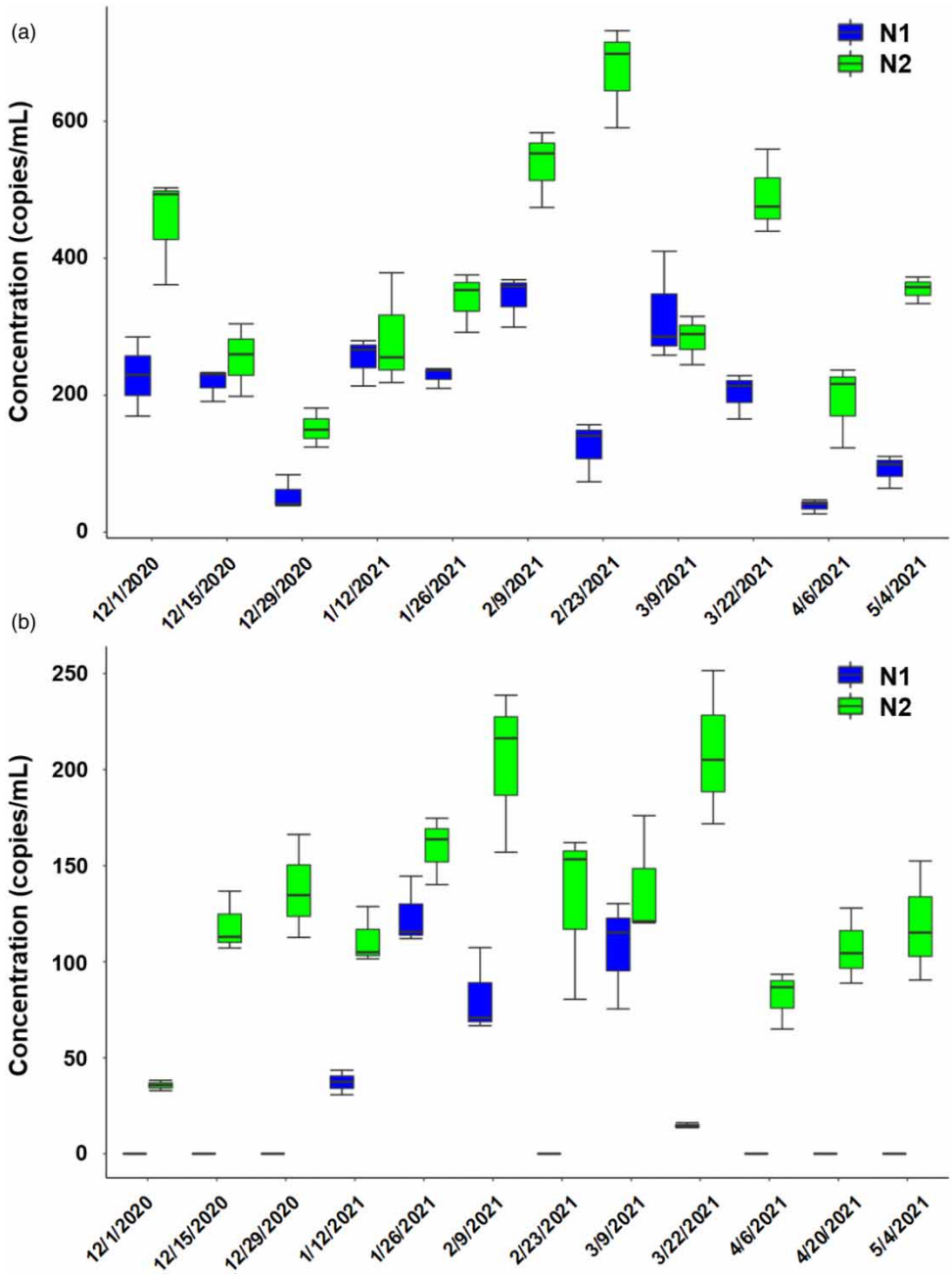

Figure 2 | The concentrations of SARS-CoV-2 N1 and N2 genes in sludge (a) and supernatant (b) samples collected from Zuma Beach RR#9. The concentrations of 0 copies/mL were used for the non-detects.

RR#1 sludge samples were recorded on December 1, 2020, with each markedly decreasing thereafter. N1 and N2 concentrations averaged 433.6 and 445.4 copies/mL, respectively, in positive RR#1 sludge samples, and 172.6 and 329.7 copies/mL, respectively, in RR#9 sludge samples. Similarly to supernatant samples, sludge N2 concentrations significantly exceeded those of N1 (Wilcoxon test, $p < 0.002$, $n = 24$). Overall, the N1 and N2 concentrations correlated with each other across supernatant and sludge samples (Spearman correlation test, $r = 0.58$ and 0.65, $p = 0.002$ and 0.001, $n = 26$ and 24, respectively).

During the sampling events when both supernatant and sludge samples were collected (seven events for RR#1 and 11 events for RR#9; Supplementary material, Table S1), the concentrations of N1 and N2 targets in sludge samples exceeded

those of the corresponding supernatant samples (Wilcoxon test, both $p = 0.0001$, $n = 18$). For these samples, sludge N1 and N2 concentrations were positively correlated with those in the corresponding supernatant samples (Spearman correlation test, $r = 0.63$ and 0.49, $p < 0.001$ and $p = 0.016$, $n = 18$ for N1 and N2, respectively).

N1 and N2 concentrations in all sludge and supernatant samples showed strong correlations with TSS values (Spearman correlation test, $r = 0.68$ and 0.51, $p = 0$ and 0.0001, $n = 46$ including both sludge and supernatant samples for N1 and N2, respectively). However, the concentrations of N1 or N2 in sludge or supernatant samples were not correlated to the 7-day average daily infection case numbers of the local city (Malibu; Supplementary material, Table S1), which might be expected given differing contributing populations. Normalized to TSS values, the average concentrations of N1 and N2 in all supernatant samples of the two RRs were 92.1 and 674.0 copies/mg TSS, respectively; the average normalized concentrations of N1 and N2 in all sludge samples were 22.5 and 44.9 copies/mg TSS, respectively.

SARS-CoV-2 depth profiles in supernatant and sludge samples

For RR#9 primary tank sludge samples collected from the top and bottom layers on March 9 and 22, 2021, all bottom sludge samples contained higher N1 and N2 concentrations (on average 231.5 and 439.3 copies/mL, respectively, $n = 4$, Supplementary material, Table S1) than corresponding top sludge samples (on average 107.3 and 151.8 copies/mL, respectively, $n = 4$) (Supplementary material, Figure S5). Similarly, all supernatant samples collected from the mid layer on March 9 and 22, 2021 contained higher N1 and N2 concentrations (on average 37.3 and 191.9 copies/mL, respectively, $n = 4$) than those in corresponding supernatant samples from the top layer (on average 0 and 71.9 copies/mL, respectively, $n = 4$) (Supplementary material, Figure S5). The higher N1 and N2 concentrations in deeper, versus shallower, supernatant and sludge layers can be explained by the correspondingly higher TSS values in deeper layers (Supplementary material, Table S1). The N2 concentration in the supernatant mid layer was similar to that in the bottom layer on April 20, 2020 (Supplementary material, Table S1).

Pumping, hauling, and discharge of septage

During the pumping and hauling sub-study of RR#9 on March 22, 2021, the average N1 and N2 concentrations were highest in sludge samples (147.3 and 333.5 copies/mL for N1 and N2, respectively, $n = 6$), followed by mixed samples after pumping (87.8 and 228.7 copies/mL, $n = 3$), mixed samples prior to discharge (29.7 and 189.3 copies/mL, $n = 3$), and supernatant samples (7.3 and 143.8 copies/mL, $n = 6$). These results suggested that some decay of SARS-CoV-2 RNA occurred during hauling of septage from Zuma Beach to JWPCP. Decay was confirmed by comparing heat-inactivated SARS-CoV-2 spiked mixed samples kept on ice with those at ambient temperature until discharge. The average N1 and N2 concentrations in triplicate spiked samples kept at ambient temperature were 5.57×10^5 and 3.97×10^5 copies/mL, respectively, which were clearly lower than those in triplicate spiked samples kept on ice (7.14×10^5 and 7.13×10^5 copies/mL, respectively). By comparing the natural log-transformed virus concentrations in septage samples collected from the haul truck just after pumping to those in samples collected just prior to discharge, the first order decay rate coefficients were 0.543 and 0.094 h^{-1} for N1 and N2, respectively (Supplementary material, Table S4). When comparing spiked septage samples kept on ice with parallel samples maintained at ambient temperature, decay coefficients for N1 and N2 were 0.124 and 0.293 h^{-1}, respectively (Supplementary material, Table S1).

PMMoV-normalized SARS-CoV-2 RNA

The PMMoV sludge concentrations (see Supplementary material) did not correspond to those in the supernatant, yet PMMoV concentrations in all supernatant and sludge samples were significantly correlated with TSS (Spearman correlation test, $r = 0.73$, $p = 0$, $n = 46$). Furthermore, for RR#1, sludge PMMoV concentrations correlated with sludge N2 concentrations (Spearman correlation test, $r = 0.96$, $p = 0.0005$, $n = 7$; Supplementary material, Table S1); for RR#9, the correlation of sludge PMMoV was with sludge N1 (Spearman correlation test, $r = 0.84$, $p = 0.001$, $n = 11$). However, supernatant PMMoV concentrations were uncorrelated with either supernatant N1 or N2, for both RRs.

After normalizing to PMMoV concentrations, all supernatant N1 and N2 averaged 0.0029 and 0.0288 copy/copy respectively; sludge N1 and N2 averaged 0.0003 and 0.0005 copy/copy, respectively. The normalized N1 and N2 concentrations remained uncorrelated with the 7-day average daily COVID-19 infection case numbers of the local city (Malibu; Supplementary material, Figures S6 and S7), again as might be expected given the differing contributing populations.

Modeled viral load and case prevalence

The measured SARS-CoV-2 loading in the sludge blanket varied over an order of magnitude during the study (Figure 3). Modeling was used to simulate the virus loading and to explore factors affecting variations in the measured data, but also to estimate the prevalence of COVID-19 disease among Zuma Beach STS users during the study period. In simulating viral loading, the modeling results were plotted as a shaded area represented by an upper estimate based on virus decay coefficient $k_d = 0.17\ d^{-1}$, the median decay estimate based on the data collected in this study (Supplementary material, Table S4), and a lower bound estimate using a higher coefficient, $k_d = 1.4\ d^{-1}$ (Figure 3(a); Ahmed *et al.* 2020; Bivins *et al.* 2020). These published decay rate constants were chosen to represent measured bounds for SARS-CoV-2 decay in wastewater from published studies. Using a representative range of decay coefficients, the model developed in this study well simulated a virus loading range that fully encompassed the measured N1 and N2 copy concentrations in the Zuma Beach STS primary tank (Figure 3(a)).

In the modeling to estimate SARS-CoV-2 loading into the STS sludge, the numbers of infected users contributing to the STS were varied based on applying assumed infection prevalence (Equation (4)) to actual measured RR#9 user counts. The prevalence of infected users that resulted in simulated virus loadings that best matched the measurements was plotted as the 7-day moving average over the study period, with the interpolation of data between sampling dates (Figure 3(b)). This prevalence, ranging from approximately 8–18% over the 5-month study period, mirrored LA County data for the first 2 months but departed and increased for the remaining period (Figure 3(b)), suggesting different patterns of infection for Zuma Beach STS users than for the nearby larger metropolitan sewered region (Figure 3(b)).

The Spearman rank sensitivity analysis indicated that the model is most sensitive to the input for virus concentration in the wastewater Z_{in} (Figure 4; Equation (3)). This parameter was drawn from a Monte Carlo simulation of clinical data, which varies over several orders of magnitude and brings greater uncertainty into the model inputs. Viral decay rate is less influential but an important contributor to the uncertainty. The viral partition in the attachment to particulates is least influential, but these parameters are still critical in modeling trends over time (Figure 4).

Relationships to regional prevalence of COVID-19 cases

The raw or normalized concentrations of SARS-CoV-2 in sludge or supernatant samples of this study, as well as a conservative estimate of disease incidence via modeling, were all uncorrelated to infection case numbers in the nearest city (Malibu: Supplementary material, Figures S6 and S7) and mostly uncorrelated to the entirety of LA County (Figure 3(b)). This owes to

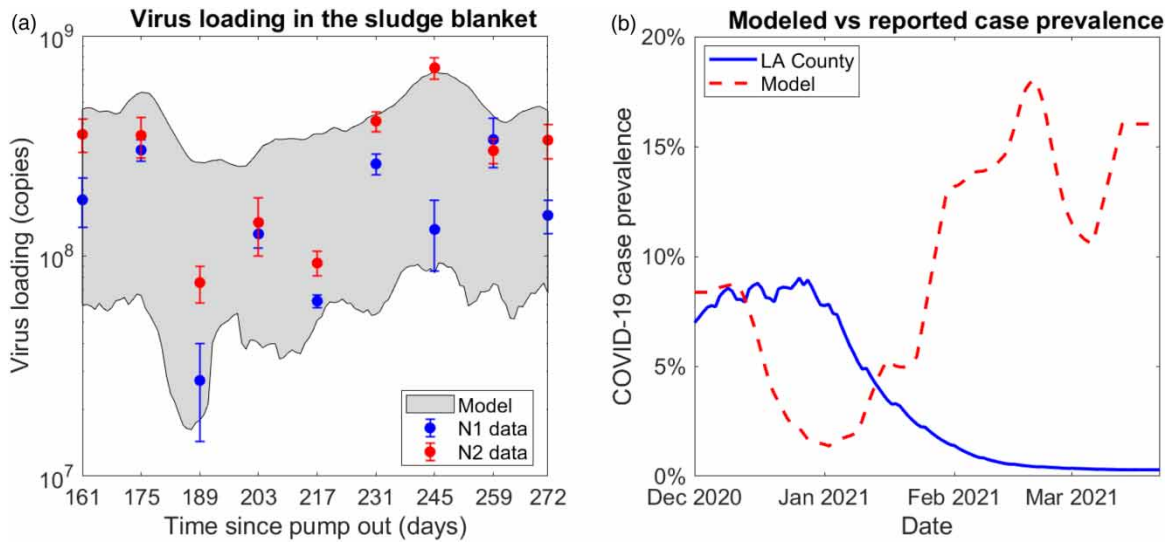

Figure 3 | Results for the modeled viral loading in the sludge blanket compared with SARS-CoV-2 measured in samples (a) and the estimated prevalence (Equation (4)) of infected individuals using RR#9 in comparison with the prevalence in LA County (Equation (5)) (b). The shaded area for (a) represents an upper estimate based on the viral decay of $k_d = 0.17\ d^{-1}$ and a lower estimate of $k_d = 1.4\ d^{-1}$(Ahmed *et al.* 2020; Bivins *et al.* 2020). Case prevalence (b) is illustrated as a 7-day moving average for both lines.

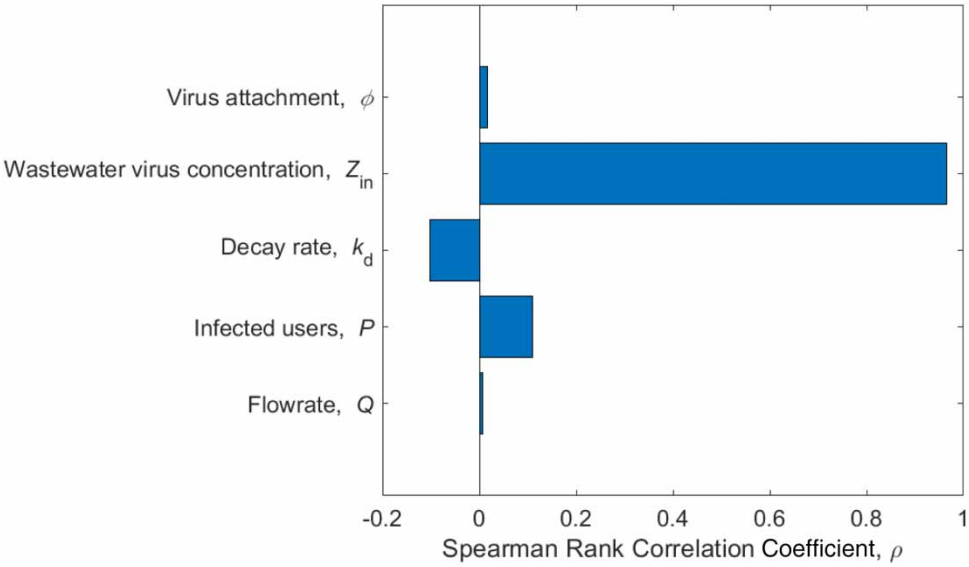

Figure 4 | Sensitivity analysis for the mass balance model (Equation (1)) and varied input parameters as defined in the 'Methods' section.

the accumulation of virus in septic samples, but also the disassociation between contributing counts of tourists and local residents in the surrounding areas. As such, directly sampling the Zuma Beach STS, or sampling the pumped hauled septage, was needed to understand SARS-CoV-2 prevalence in users.

DISCUSSION

Many studies have monitored SARS-CoV-2 RNA in WWTP influent or primary sludge (Graham *et al.* 2020; Medema *et al.* 2020), showing good correlations to local infection cases (Graham *et al.* 2020). However, unsewered areas are served by STSs or by communal holding tanks in developing countries, with each type of system being periodically pumped. In contrast to centralized (sewered) systems, decentralized WWS is currently overlooked in pandemic prevention (Shrestha *et al.* 2021; Chigwechokha *et al.* 2022), although some investigations into holding tanks were performed previously to understand community health (Capone *et al.* 2021). The few reports of SARS-CoV-2 RNA in STSs until now determined the presence of SARS-CoV-2 RNA in septic tanks (Zhang *et al.* 2020; Iwamoto *et al.* 2022; Amin *et al.* 2023), including detecting virus RNA after disinfection with sodium hypochlorite (Zhang *et al.* 2020).

STSs can be effective in treating household wastewater, although they can pollute groundwater and surface waters with excess nitrogen, phosphorus, and pathogens (Withers *et al.* 2014; Lusk *et al.* 2017). Viruses are of the greatest concern due to their ineffective removal by STSs and long-term survival in soil (Ferguson *et al.* 2009). The source of viruses to STSs is human feces, and so septage viral concentrations reflect the infection of served residents. However, where and how to sample STSs or communal holding systems for SARS-CoV-2 is relatively unknown (Haque *et al.* 2022), including if representative sampling can conveniently be performed during system pump-out. Furthermore, how to use pathogen detections from septage or holding tank wastewater for WWS is largely unexplored. Given the extensive use of STSs and similar decentralized sanitation systems in rural areas or areas of low population density, and the preponderance of similar holding and transport conditions for wastewater in developing countries (Maqbool *et al.* 2022), studying STSs for SARS-CoV-2 can assist with planning how to apply WWS principles to SARS-CoV-2 outside of sewered areas. Examining the main septage compartments, i.e., supernatant and sludge, for SARS-CoV-2 distribution, as well as determining the feasibility and representativeness of system pump-out for sampling SARS-CoV-2, is a first step toward defining STS WWS. This study was thus aimed at determining where and how to sample STSs, which required using comparable and consistent analytical methods across sample compartments and stages such as holding or transporting (Maqbool *et al.* 2022), and how to use the data for WWS. Considering that most household STSs cannot be easily accessed for sampling, STSs such as those serving two high-use public restrooms located at Zuma Beach were studied here.

The PMMoV-normalized SARS-CoV-2 concentrations in STS primary tank supernatant and sludge samples of this study were in similar ranges to those reported elsewhere for WWTP influent and sludge (Graham *et al.* 2020). Also, the results of this study mirrored findings of WWTP studies in which primary clarified sludge samples had higher SARS-CoV-2 detection frequencies and concentrations relative to corresponding WWTP influent samples (Graham *et al.* 2020; Balboa *et al.* 2021; D'Aoust *et al.* 2021). SARS-CoV-2 is an enveloped virus which contains a lipid bilayer membrane (envelope) surrounding the protein capsid, resulting in relatively effective sorption onto solid residues in wastewater compared to non-enveloped viruses (Kitajima *et al.* 2020). This explains the higher accumulation of SARS-CoV-2 in sludge versus supernatant samples, and the correlation between SARS-CoV-2 RNA and TSS in this study.

Still, how SARS-CoV-2 is quantified, i.e., which target is assessed, may change the impression of viral loading. Assays for N2 are reportedly more sensitive compared to those for N1 (Nalla *et al.* 2020). Wastewater or sludge concentrations of N1 and N2 have been reported as correlated (Peccia *et al.* 2020), but other studies of N1 and N2 genes report discrepancies, such as both targets never co-detected in influent samples (Graham *et al.* 2020), or no correlation between their concentrations (D'Aoust *et al.* 2021). In our study, N2 concentrations exceeded those for N1 in both supernatant and sludge samples, while their concentrations were still significantly correlated with each other.

Ageing of wastewater will also affect SARS-CoV-2 assessments, and here relates to two concerns: 1) how well STS SARS-CoV-2 represents community virus loads given that wastewater in STSs is stored, and 2) the extent to which SARS-CoV-2 decays upon sampling of STSs. Related to the first concern, during wastewater storage in septic tanks, solids settling in supernatant and sludge concentrates the solids-associated virus into deep versus shallow compartment layers, as evidenced by the supernatant and sludge SARS-CoV-2 depth profiles (Supplementary material, Figure S5). Then, wastewater in STSs, particularly the sludge, is held before pumping out and hauling for disposal. This is in contrast to primary sludge in WWTPs with retention times on the order of days (Metcalf & Eddy 2014). Overall STS SARS-CoV-2 decay might therefore exceed that in WWTP influent or primary clarifier sludge. Here, this was evidenced by low ratios of N1 and N2 sludge concentrations relative to supernatant concentrations as compared to N1 and N2 concentrations on a per mass basis reportedly being 100 to 1,000 times higher in primary clarifier solids compared to wastewater (Graham *et al.* 2020). For the second concern, previous studies of wastewater suggested that SARS-CoV-2 RNA decay followed a first order process, with decay rate coefficients ranging from 0.09 to 0.12 h^{-1}, and temperature expectedly influencing the values (Ahmed *et al.* 2020; Guo *et al.* 2023). Furthermore, slower decay of viral RNA targets was reported in primary settled solids when comparing to wastewater influent (Roldan-Hernandez *et al.* 2022), suggesting that SARS-CoV-2 RNA can be more persistent in solids. Here, beyond the storage time in the STS, decay coefficients during the pumping and hauling were in accordance with other reported values at the same temperature (25 °C) (Guo *et al.* 2023). Overall, both the length of sludge storage time in STSs, plus the act of sampling, can impair accurate assessments of SARS-CoV-2 in STS wastewater. Regardless, where STSs are in use, such as at least daily at the household level or more frequently at the communal level, input of wastewater by infected users coupled with the sensitive detection of either N1 or N2 gene copies suggests that the STS or communal tank wastewater holds pathogen content of use for WWS.

How to apply STS or communal waste sampling for SARS-CoV-2 for WWS is of importance and thus also motivated the modeling work in this study. Considering the large number of STSs in residential or rural communities – and of similarly functioning holding tanks in developing countries, 'spot tests' of selected STSs may be impractical for understanding the circulation of virus in the community due to the cost and the fact that most household STSs cannot be easily accessed for sampling. In contrast, sampling for the virus from the hauler, such as at the point of disposal at the WWTP that received the septage, is practical. Although large STSs accessible to the public were investigated in this study, in most cases the pumped septage would be from selected individual septic systems in a rural community. Thus, testing from the hauler can potentially reveal 'hot spots' of infection across expansive rural areas. In concept, a possible WWS strategy for a model city that has 750 STSs – spanning inside the urban boundary and nearby but external to the city boundary – is as follows. The city is assumed to have 100,000 residences total, with most properties connected to a sewer system served by a WWTP. Yet approximately 0.4% of city properties are served by STSs, and a similar number use STSs in less densely-developed regions that are nearby but external to the urban boundary (Figure 5). For this total of approximately 750 STSs that are within a few miles of the WWTP to which septage would be pumped approximately every 5 years and hauled for disposal (U.S. EPA 1994), pumping and hauling is assumed to occur 50 weeks per year, thus averaging three STSs pumped during 1 day per week by a single truck. This is reasonable, considering that one haul truck would have a capacity of approximately 4,000 gallons and each STS tank is approximately 1,000 gallons (U.S. EPA 1994). During each of two example sampling

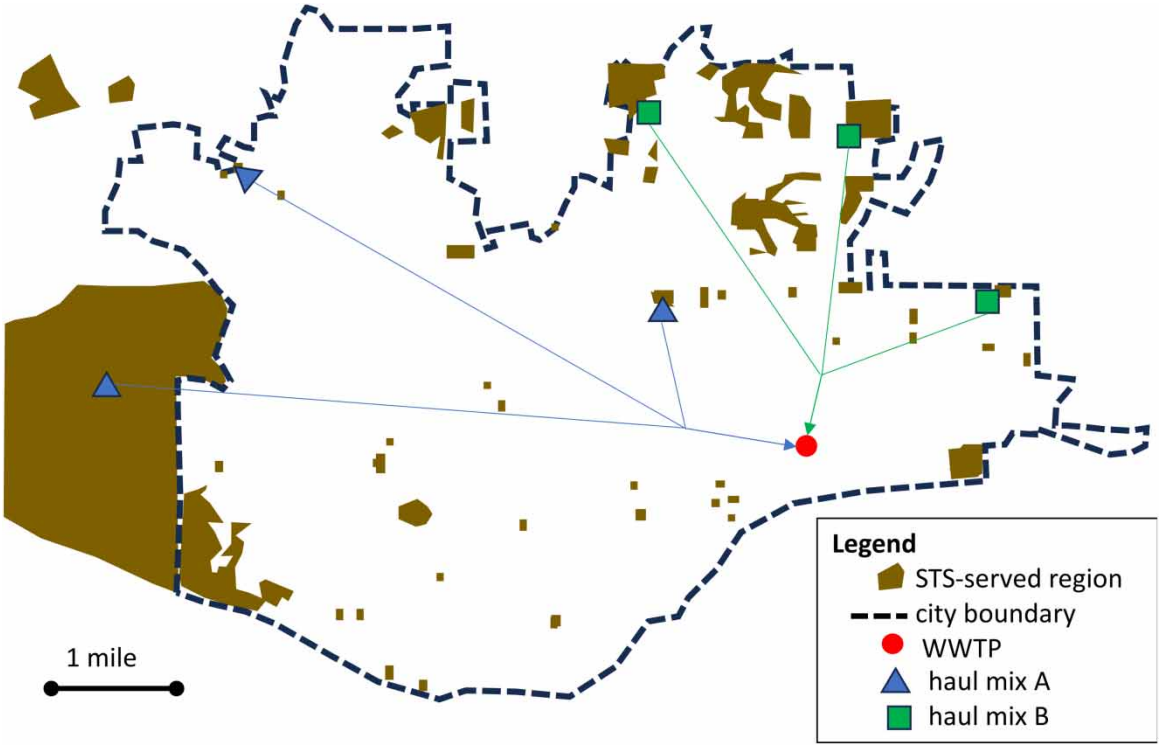

Figure 5 | Conceptual model of a city that has STSs inside the city boundary, as well as outside but nearby, showing the spatial coverage of STS pumping and hauling over a putative 2-week period, where haul mix A retrieves – in a single serial haul – septage from three pumped STSs (blue triangles), and haul mix B retrieves from three different pumped STSs (green rectangles) during a successive week. Fine lines with arrows indicate that the three sampled STSs each week are composited as a single truck pumps from each site serially before hauling the composite of the three pumped STSs' septage to the WWTP (red circle). The exact STS locations are known by the pumper and hauler, making a composite sample from disposed truck contents at the WWTP nearly spatially resolved, thus complementing typical WWS of WWTP influent which composites across the entire collection system within the sewered city boundary (dotted black line). For example, a surveilled pathogen detection in haul mix A may motivate sampling within the city collection system near the STS of that haul mix that is within the city boundary. Similar steps could be decided for haul mix B. For other conceptual haul mixes that might occur from pumping only from STSs outside the city boundary, public health protection recommendations may be amplified to rural residents since rural disease hotspots would be evidenced. This conceptual model is based on an actual city near the study site of this research as described in Supplementary material. Please refer to the online version of this paper to see this figure in colour: https://dx.doi.org/10.2166/wh.2023.128.

weeks with different spatial coverages of pumped STSs (Figure 5), the WWTP – in addition to its ongoing WWS of WWTP influent and/or primary solids – samples from the outlet of the hauling truck during septage disposal. Analysis of the pathogens in this septic haul sample would reveal pathogen detections for a composite of three STSs. The spatial resolution by analyzing this septage sample provides regional public health and WWS managers with crucial information: if the pathogen of concern has occurred in the pumped STSs. While such sampling and analysis only 'spot checks' those STSs that are sampled, any detections provide clear evidence of where disease might be spreading in the community, perhaps giving a finer spatial view even earlier in a potential pandemic than is afforded by only monitoring the WWTP influent for sewered community WWS.

Surveillance of STSs would be adaptable to localized needs and could include diverse human pathogens such as *Vibrio cholerae* or poliovirus, besides SARS-CoV-2 (Chigwechokha *et al.* 2022). Targeted clinical testing could be implemented by local public health officials, based on such WWS of septic systems. The epidemiology of regional human pathogens and early warnings of a pandemic can be obtained by combining WWS of STSs, relative to WWS of nearby sewered areas, with clinical data of circulating disease. Furthermore, given that WWS of STSs has the potential to, relative to WWS at WWTPs, spatially pinpoint positive disease detects earlier, i.e., before a sewerage utility might decide to extend WWS from the WWTP influent upstream into the collection system, where to direct public health interventions could also be informed by STS- or communal holding tank-based WWS.

CONCLUSIONS

The sampling work in this study demonstrated that septic solids, or pumped and hauled septage, are suitable for sampling and assessment of SARS-CoV-2. The results of this study add insights regarding SARS-CoV-2 RNA in STSs, demonstrate viral distribution within STSs, and show how to sample including conveniently during pumped septage hauling. The modeling results further demonstrate the ability to scale and predict virus accumulation in an STS pumped out regularly, and to estimate the amount of SARS-CoV-2 infection among STS users. Practical WWS strategies for SARS-CoV-2 or other human pathogens based on pumped septage sampling and modeling are informed by this research for septic systems or communal holding tanks in unsewered communities, perhaps even as a complement to ongoing WWTP WWS of influent in the same region.

ACKNOWLEDGEMENTS

This study was supported by the Water Research Foundation project 5093. P.A.H. acknowledges support from the UCSB AS Coastal Fund. S.J. is also supported by U.S. National Science Foundation CBET 2027306, CBET 2128480, CBET 1806066, USBR R21AC10079-00, and EPA (EPA-G2021-STAR-A1, Grant number: 84025701). The contents of this document do not necessarily reflect the views and policies of the U.S. NSF, EPA, USBR, nor does the agencies endorse trade names or recommend the use of any commercial products mentioned in this document. We are grateful for the support of UCI Water-Energy Nexus Center for sampling and coordination with local water utilities.

AUTHOR CONTRIBUTIONS

D.L. and H.Q. contributed equally to this paper. D.L. did sample analysis and paper writing; H.Q. did modeling and paper writing; J.E. did research design and field sampling; S.J. did project management, research design, paper editing; D.R. did modeling and paper editing; L.C.V.D.W. did sample analysis, paper editing; B.S. did research design, project coordination and paper editing. P.A.H. did research design, project coordination, and paper writing and editing.

DATA AVAILABILITY STATEMENT

All relevant data are included in the paper or its Supplementary material.

CONFLICT OF INTEREST

The authors declare there is no conflict.

REFERENCES

Ahmed, W., Bertsch, P. M., Bibby, K., Haramoto, E., Hewitt, J., Huygens, F., Gyawali, P., Korajkic, A., Riddell, S., Sherchan, S. P., Simpson, S. L., Sirikanchana, K., Symonds, E. M., Verhagen, R., Vasan, S. S., Kitajima, M. & Bivins, A. 2020 Decay of SARS-CoV-2 and surrogate murine hepatitis virus RNA in untreated wastewater to inform application in wastewater-based epidemiology. *Environ. Res.* **191**, 110092.

Amin, N., Haque, R., Rahman, M. Z., Rahman, M. Z., Mahmud, Z. H., Hasan, R., Islam, M. T., Sarker, P., Sarker, S., Adnan, S. D., Akter, N., Johnston, D., Rahman, M., Liu, P., Wang, Y., Shirin, T., Rahman, M. & Bhattacharya, P. 2023 Dependency of sanitation infrastructure on the discharge of faecal coliform and SARS-CoV-2 viral RNA in wastewater from COVID and non-COVID hospitals in Dhaka, Bangladesh. *Sci. Total Environ.* **867**, 161424.

Balboa, S., Mauricio-Iglesias, M., Rodriguez, S., Martínez-Lamas, L., Vasallo, F. J., Regueiro, B. & Lema, J. M. 2021 The fate of SARS-COV-2 in WWTPS points out the sludge line as a suitable spot for detection of COVID-19. *Sci. Total Environ.* **772**, 145268.

Bivins, A., Greaves, J., Fischer, R., Yinda, K. C., Ahmed, W., Kitajima, M., Munster, V. J. & Bibby, K. 2020 Persistence of SARS-COV-2 in water and wastewater. *Environ. Sci. Technol. Lett.* **7**, 937–942.

Capone, D., Chigwechokha, P., de Los Reyes 3rd, F. L., , Holm, R. H., Risk, B. B., Tilley, E. & Brown, J. 2021 Impact of sampling depth on pathogen detection in pit latrines. *PLoS Negl. Trop. Dis.* **15**, e0009176.

CDC 2021 *Estimated Covid-19 Burden*. Centers for Disease Control and Prevention. Retrieved October 19, 2022. Available from: https://www.cdc.gov/coronavirus/2019-ncov/cases-updates/burden.html

Chigwechokha, P., Street, R. & Holm, R. H. 2022 Advancing the use of fecal sludge for timelier and better-quality epidemiological data in low- and middle-income countries for pandemic prevention. *Environ. Sci. Technol.* doi:10.1021/acs.est.2c07788.

D'Aoust, P. M., Mercier, E., Montpetit, D., Jia, J. J., Alexandrov, I., Neault, N., Baig, A. T., Mayne, J., Zhang, X., Alain, T. & Langlois, M. A. 2021 Quantitative analysis of SARS-CoV-2 RNA from wastewater solids in communities with low COVID-19 incidence and prevalence. *Water Res.* **188**, 116560.

Diamond, M. B., Keshaviah, A., Bento, A. I., Conroy-Ben, O., Driver, E. M., Ensor, K. B., Halden, R. U., Hopkins, L. P., Kuhn, K. G., Moe, C. L., Rouchka, E. C., Smith, T., Stevenson, B. S., Susswein, Z., Vogel, J. R., Wolfe, M. K., Stadler, L. B. & Scarpino, S. V. 2022 Wastewater surveillance of pathogens can inform public health responses. *Nat. Med.* **28**, 1992–1995.

Ferguson, C. M., Charles, K. & Deere, D. A. 2009 Quantification of microbial sources in drinking water catchments. *Crit. Rev. Environ. Sci. Technol.* **39**, 1–40.

Gernaey, K., Vanrolleghem, P. A. & Lessard, P. 2001 Modeling of a reactive primary clarifier. *Water Sci. Technol.* **43**, 73–81.

Graham, K. E., Loeb, S. K., Wolfe, M. K., Catoe, D., Sinnott-Armstrong, N., Kim, S., Yamahara, K. M., Sassoubre, L. M., Mendoza Grijalva, L. M., Roldan-Hernandez, L. & Langenfeld, K. 2020 SARS-CoV-2 RNA in wastewater settled solids is associated with COVID-19 cases in a large urban sewershed. *Environ. Sci. Technol.* **55**, 488–498.

Guo, Y., Liu, Y., Gao, S., Zhou, X., Sivakumar, M. & Jiang, G. 2023 Effects of temperature and water types on the decay of coronavirus: a review. *Water* **15**, 1051.

Haque, R., Moe, C. L., Raj, S. J., Ong, L., Charles, K., Ross, A. G., Shirin, T., Raqib, R., Sarker, P., Rahman, M., Rahman, M. Z., Amin, N., Mahmud, Z. H., Rahman, M., Johnston, D., Akter, N., Khan, T. A., Hossain, M. A., Hasan, R., Islam, M. T. & Bhattacharya, P. 2022 Wastewater surveillance of SARS-CoV-2 in Bangladesh: opportunities and challenges. *Curr. Opin. Environ. Sci. Health* **27**, 100334.

Iwamoto, R., Yamaguchi, K., Arakawa, C., Ando, H., Haramoto, E., Setsukinai, K. I., Katayama, K., Yamagishi, T., Sorano, S., Murakami, M., Kyuwa, S., Kobayashi, H., Okabe, S., Imoto, S. & Kitajima, M. 2022 The detectability and removal efficiency of SARS-CoV-2 in a large-scale septic tank of a COVID-19 quarantine facility in Japan. *Sci. Total Environ.* **849**, 157869.

Kitajima, M., Ahmed, W., Bibby, K., Carducci, A., Gerba, C. P., Hamilton, K. A., Haramoto, E. & Rose, J. B. 2020 SARS-CoV-2 in wastewater: state of the knowledge and research needs. *Sci. Total. Environ.* **739**, 139076.

Lusk, M. G., Toor, G. S., Yang, Y. Y., Mechtensimer, S., De, M. & Obreza, T. A. 2017 A review of the fate and transport of nitrogen, phosphorus, pathogens, and trace organic chemicals in septic systems. *Crit. Rev. Environ. Sci. Technol.* **47**, 455–541.

Maqbool, N., Shahid, M. A. & Khan, S. J. 2022 Situational assessment for fecal sludge management in major cities of Pakistan. *Environ. Sci. Pollut. Res. Int.* **9**, 1–12.

Massoud, M. A., Tarhini, A. & Nasr, J. A. 2009 Decentralized approaches to wastewater treatment and management: applicability in developing countries. *J Environ. Manage.* **90**, 652–659.

MATLAB 2022 *version 9.12.0 (R2022a)*. The MathWorks Inc, Natick, Massachusetts.

Medema, G., Heijnen, L., Elsinga, G., Italiaander, R. & Brouwer, A. 2020 Presence of SARS-Coronavirus-2 in sewage and correlation with reported COVID-19 prevalence in the early stage of the epidemic in The Netherlands. *Environ. Sci. Technol. Lett.* **7**, 511–516.

Metcalf & Eddy Inc., Tchobanoglous, G., Burton, F. L., Tsuchihashi, R. & Stensel, H. D. 2014 *Wastewater Engineering: Treatment and Resource Recovery*, 5th edn. McGraw-Hill Professional, New York, p. 2048.

Nalla, A. K., Casto, A. M., Huang, M. L. W., Perchetti, G. A., Sampoleo, R., Shrestha, L., Wei, Y., Zhu, H., Jerome, K. R. & Greninger, A. L. 2020 Comparative performance of SARS-CoV-2 detection assays using seven different primer-probe sets and one assay kit. *J Clin. Microbiol.* **58**, e00557–20.

Nishiura, H., Kobayashi, T., Miyama, T., Suzuki, A., Jung, S. M., Hayashi, K., Kinoshita, R., Yang, Y., Yuan, B., Akhmetzhanov, A. R. & Linton, N. M. 2020 Estimation of the asymptomatic ratio of novel coronavirus infections (COVID-19). *Int. J Infect. Dis.* **94**, 154–155.

Peccia, J., Zulli, A., Brackney, D. E., Grubaugh, N. D., Kaplan, E. H., Casanovas-Massana, A., Ko, A. I., Malik, A. A., Wang, D., Wang, M., Warren, J. L., Weinberger, D. M., Arnold, W. & Omer, S. B. 2020 Measurement of SARS-CoV-2 RNA in wastewater tracks community infection dynamics. *Nat. Biotechnol.* **38**, 1164–1167.

Roldan-Hernandez, L., Graham, K. E., Duong, D. & Boehm, A. B. 2022 Persistence of endogenous SARS-CoV-2 and pepper mild mottle virus RNA in wastewater-settled solids. *ACS EST Water.* **2**, 1944–1952.

Shi, K. W., Huang, Y. H., Quon, H., Ou-Yang, Z. L., Wang, C. & Jiang, S. C. 2021 Quantifying the risk of indoor drainage system in multi-unit apartment building as a transmission route of SARS-CoV-2. *Sci. Total Environ.* **762**, 143056.

Shrestha, S., Yoshinaga, E., Chapagain, S. K., Mohan, G., Gasparatos, A. & Fukushi, K. 2021 Wastewater-based epidemiology for cost-effective mass surveillance of COVID-19 in low- and middle-income countries: challenges and opportunities. *Water* **13**, 2897.

Takács, I., Patry, G. G. & Nolasco, D. 1991 A dynamic model of the clarification-thickening process. *Water Res.* **25**, 1263–1271.

U.S. EPA 1994 *Guide to Septage Treatment and Disposal.* EPA 625/R-94/002. U. S. Environmental Protection Agency, Office of Research and Development, Washington, D. C.

U.S. EPA 2002 *Onsite Wastewater Treatment Systems Manual.* EPA 625/R-00/008. U. S. Environmental Protection Agency, Office of Research and Development, Washington, D. C.

Williams, R., Keller, V., Voß, A., Bärlund, I., Malve, O., Riihimäki, J., Tattari, S. & Alcamo, J. 2012 Assessment of current water pollution loads in Europe: estimation of gridded loads for use in global water quality models. *Hydrol. Process* **26**, 2395–2410.

Withers, P. J., Jordan, P., May, L., Jarvie, H. P. & Deal, N. E. 2014 Do septic tank systems pose a hidden threat to water quality? *Front. Ecol. Environ.* **12**, 123–130.

Wölfel, R., Corman, V. M., Guggemos, W., Seilmaier, M., Zange, S., Müller, M. A., Niemeyer, D., Jones, T. C., Vollmar, P., Rothe, C. & Hoelscher, M. 2020 Virological assessment of hospitalized patients with COVID-2019. *Nature* **581**, 465–469.

Wyman, J. B., Heaton, K. W., Manning, A. P. & Wicks, A. C. 1978 Variability of colonic function in healthy subjects. *Gut* **19**, 146–150.

Ye, Y., Ellenberg, R. M., Graham, K. E. & Wigginton, K. R. 2016 Survivability, partitioning, and recovery of enveloped viruses in untreated municipal wastewater. *Environ. Sci. Technol.* **50**, 5077–5085.

Zhang, D., Ling, H., Huang, X., Li, J., Li, W., Yi, C., Zhang, T., Jiang, Y., He, Y., Deng, S. & Zhang, X. 2020 Potential spreading risks and disinfection challenges of medical wastewater by the presence of severe acute respiratory syndrome coronavirus 2 (SARS-CoV-2) viral RNA in septic tanks of Fangcang Hospital. *Sci. Total Environ.* **741**, 140445.

Zheng, S., Fan, J., Yu, F., Feng, B., Lou, B., Zou, Q., Xie, G., Lin, S., Wang, R., Yang, X. & Chen, W. 2020 Viral load dynamics and disease severity in patients infected with SARS-CoV-2 in Zhejiang province, China, January-March 2020: retrospective cohort study. *BMJ* **369**, m1443.

First received 17 May 2023; accepted in revised form 24 August 2023. Available online 6 September 2023